# Fabrication and Properties of Dense *Ex Situ* Magnesium Diboride Bulk Material using Spark Plasma Sintering

C.E.J. Dancer[1], D. Prabhakaran[2], M. Başoğlu[3], E. Yanmaz[3], H. Yan[4], M. Reece[4], R.I. Todd[1], C.R.M. Grovenor[1]

[1] Department of Materials, University of Oxford, Parks Road, Oxford, OX1 3PH, UK
[2] Department of Physics, University of Oxford, Clarendon Laboratory, Parks Road, Oxford, OX1 3PU, UK
[3] Department of Physics, Faculty of Arts and Sciences, Karadeniz Technical University, 61080 Trabzon, Turkey
[4] Department of Materials, Queen Mary, University of London, Mile End Road, London, E1 4NS, UK

Email: claire.dancer@linacre.oxon.org

**Abstract.** High density *ex situ* magnesium diboride bulks were synthesized from commercial $MgB_2$ powder using spark plasma sintering under a range of applied uniaxial pressures between 16 and 80 MPa. The microstructure was characterized using x-ray diffraction, scanning electron microscopy, polarized optical microscopy, Vickers hardness measurements, and density measurements using the Archimedes method. By combining these data with those for other bulk samples we have developed a correlation curve for the hardness and density for magnesium diboride for relative densities of 60–100%. The superconducting properties were determined using magnetization measurements. Comparison to samples of significantly higher porosity indicates a positive correlation between magnetization critical current density and bulk density for magnesium diboride bulks up to around 90% density. Above this level other microstructural processes such as grain growth begin to influence the critical current density, suggesting that full elimination of porosity is not necessary to obtain high critical current density. We conclude that the best superconducting properties are likely to be obtained with a combination of small grain size and minimal porosity.

## 1. Introduction

Since the discovery of superconductivity in magnesium diboride in 2001 [1], wires, tapes, thin films and bulks have been produced using both the *in situ* method with a variety of precursors and the *ex situ* method using $MgB_2$ starting powder [2-4]. In contrast to the more often studied *in situ* processing route, *ex situ* processing does not result in a large density change since there is little reaction during heat-treatment, and impurity formation can be limited by adjusting the temperature and duration of

the heat-treatment. During *in situ* $MgB_2$ processing, an increase in density on formation of $MgB_2$ from Mg and B powders from 2.1 g/cm$^3$ for the powder mixture to 2.63 g/cm$^3$ for the $MgB_2$ phase occurs [5] leading to greater porosity in the final sample, and restricting the maximum final density of the artefact to around 80 % of the density of $MgB_2$ as calculated from the lattice parameters (2.63 g/cm$^3$). *Ex situ* processing is therefore the preferred method of at least one major industrial team for the commercial production of powder-in-tube (PIT) wires [6].

A positive correlation between sample density and onset transition temperature $T_{c,0}$ has been established by Grinenko *et al.* who studied $MgB_2$ bulks with densities between 16-70% of the maximum density [7]. $MgB_2$ bulks with significantly higher density have been produced by pressure-assisted heat-treatments such as hot isostatic pressing (HIPing) [8-13], hot-pressing [14-16], and spark plasma sintering (SPS) [17-19]. However there has been limited exploration of the effect of varying key processing parameters during these procedures on the subsequent density, connectivity and superconducting properties of the material.

This work examines the key parameters in the production of dense magnesium diboride, specifically by determining the effect of pressure and atmosphere on the microstructure and superconducting properties of $MgB_2$ bulks produced by SPS. This technique combines uniaxial applied pressure with high temperature heating obtained by passing direct current through a graphite die in a controlled atmosphere.

## 2. Experimental methods

All samples studied in this work were prepared using Alfa Aesar $MgB_2$ powder (98 % purity, -325 mesh). Characterization of this powder including particle size distribution and morphology was discussed in our previous paper [20]. The batch of $MgB_2$ powder used for these samples has a $\theta$-$2\theta$ X-ray diffraction (XRD) spectrum consisting solely of peaks attributable to the $MgB_2$ phase.

The ceramics were processed using a SPS furnace (Model HPD25/1, manufactured by FCT Systeme GmbH, Germany). A schematic diagram of the SPS furnace is shown in figure 1. $MgB_2$ powder was poured into a graphite die lined with graphite paper, and the powder compacted into a pellet using a uniaxial press. This was then placed in the SPS chamber and heated by passing high pulsed direct current through the die via the upper and lower rams, with simultaneous application of uniaxial pressure. Samples were produced at different applied uniaxial pressures (16, 50 and 80 MPa) since the effect of this processing parameter has received least attention in previous work, to a maximum temperature of 1250 $^{o}$C, and either in vacuum or under high-purity argon gas. The ram displacement, temperature, and pressure were recorded during the heat-treatment.

Following heat-treatment, the graphite paper and the carbon-contaminated surface layers were removed from the samples using a flat bed grinder. The density of the samples was then measured using the Archimedes method with propan-2-ol as the immersion medium. The hardness was measured at room temperature by Vickers indentation with a 2 kg load and a 10 s dwell time. To identify any impurity phases formed during heat-treatment, XRD was carried out on all samples using a Philips $\theta$-$2\theta$ diffractometer with Cu-$K_\alpha$ radiation generated at 35 kV and 50 mA. The increase in MgO content during heat-treatment was quantified by comparing the ratio of the peak areas of the $MgB_2$ (110) and MgO (220) peaks in the $\theta$-$2\theta$ X-ray diffraction spectrum for known standards to those of each sample, as described in [20]. Small sections were cut from the bulk pellets using an oil-cooled diamond slow saw and

polished in a series of stages using non-aqueous diamond polishing pastes with diamond particle sizes ranging from 45 μm to 0.1 μm. Polarised optical microscopy was carried out on these polished sections using an Olympus BX60M polarizing optical microscope. Samples were also fractured and these fracture surfaces examined using a JEOL 840F scanning electron microscope with a field-emission gun operated at 5 kV.

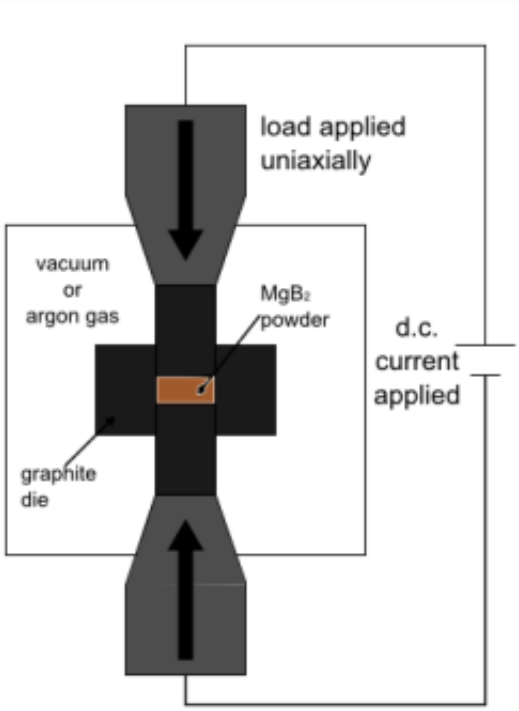


**Figure 1.** Schematic diagram of the spark plasma sintering apparatus.

Magnetization measurements were carried out on selected samples cut using an oil-cooled saw into cuboids with typical dimensions of approximately 2.3x1.9x2.0 $mm^3$. Measurements were carried out at constant temperatures (4 K and 20 K) in a changing magnetic field between -6 T and 6 T by a vibrating sample magnetometer (VSM) module in a Quantum Design Systems Physical Properties Measurement System (PPMS) model 6000 using a sweep rate of 30 Oe/s. All measurements were carried out in the zero-field cold (ZFC) regime whereby the system is cooled under with no applied field, and between measurements at different temperatures the temperature is raised to 50 K and the field to 1000 Oe to remove trapped field inside the sample. The field is then reduced to zero and the temperature set to the desired value.

## 3. Results and Discussion

Plots of temperature, applied uniaxial pressure and ram displacement recorded during the SPS cycle are shown in figure 2 for samples heat-treated in vacuum at applied uniaxial pressures of 16, 50 and 80 MPa, and under Ar gas at applied uniaxial pressure of 80 MPa. The maximum distance travelled by the ram throughout the SPS cycle increased with applied pressure for all samples. For the sample produced at 80 MPa in vacuum (figure 2(a)), densification (as indicated by a rapid change in the ram

displacement) occurs in two identifiable steps. The first occurs just before the maximum pressure is reached at around 400°C, which is significantly lower than the expected sintering temperature for a classical ceramic (typically 50–75% of the melting point) [21]. Comparison to the samples produced at lower applied pressures (Figures 2b-c) shows that the extent of this displacement step varies according to the pressure applied. Therefore we conclude that this first stage is due to cold compaction of the powder rather than true densification. Around 800-900°C for the sample produced at 80 MPa pressure some increase in ram displacement is seen; this is due to thermal expansion of the die. Similar behaviour is seen for the other samples produced in vacuum. As the temperature increases above 1000°C, another rapid decrease in ram displacement is observed, which we believe to be the onset of true sintering, and is observed in all samples. This temperature is similar to that observed by Tampieri *et al*, who found an onset sintering temperature of 1050°C for hot pressing under 30 MPa uniaxial pressure in vacuum [15].

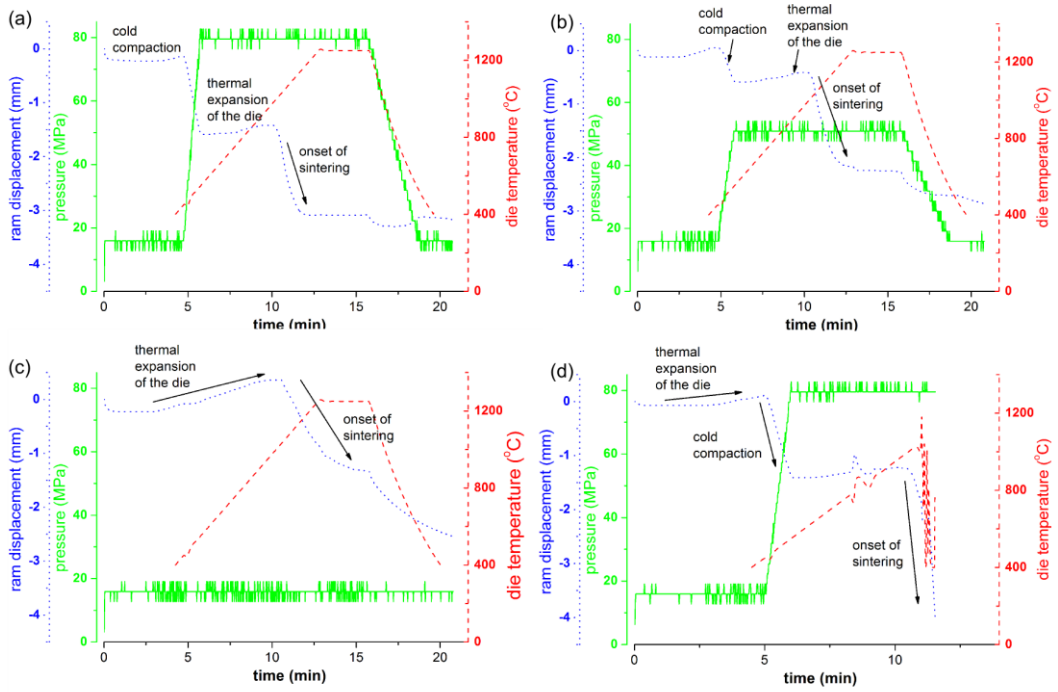


**Figure 2.** Temperature, uniaxial pressure and ram displacement logged during spark plasma sintering under vacuum and maximum applied pressures of (a) 80 MPa (b) 50 MPa and (c) 16 MPa, and (d) in Ar gas under maximum applied pressure of 80 MPa.

Another sample was produced in the same way and heat-treated under argon gas at applied uniaxial pressure of 80 MPa. This heat-treatment was stopped at 1000 °C due to a very rapid and sudden drop in the ram displacement believed to be due to impurity formation during heat-treatment, possibly due to reaction with residual oxygen in the argon gas system (see Figure 2d). $\theta$-$2\theta$ XRD indicated that this sample consisted almost entirely of MgO (Figure 3 and Table 1). The recently updated phase diagram for Mg–B system [22] indicates that at these processing temperatures Mg vapour is present in equilibrium with $MgB_2$ or $MgB_4$, therefore it is possible that the MgO forms by reaction of Mg vapour with residual oxygen in the argon gas system (see figure 2(d)).

The numerical densities of the two samples spark plasma sintered at 80 MPa and 50 MPa were 2.65 g/cm$^3$, which is within experimental error identical to the maximum theoretical density of pure $MgB_2$ calculated from the lattice parameters (2.63 g/cm$^3$). The numerical density of the samples spark plasma sintered at 16 MPa in vacuum and at 80 MPa in Ar gas were 2.52 g/cm$^3$ and 2.21 g/cm$^3$ respectively. However, it is not reasonable to compare these figures directly to the theoretical maximum density of pure $MgB_2$ without considering the impurity content of the samples.

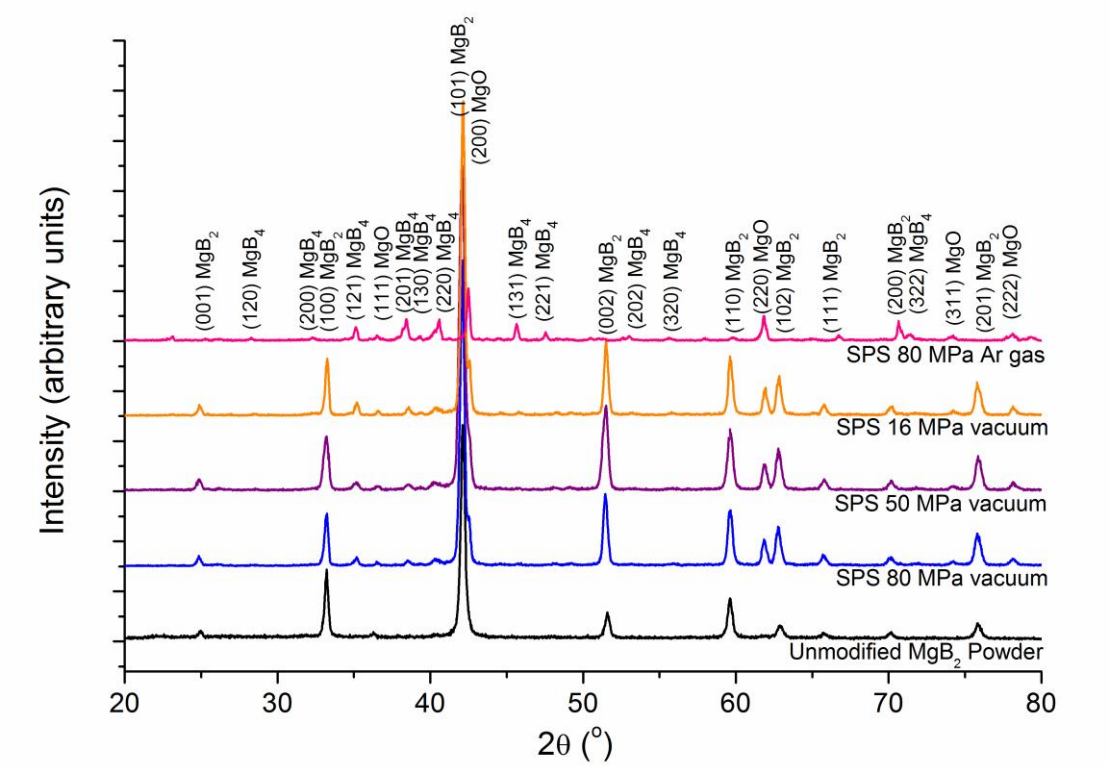


**Figure 3.** X-ray diffraction spectra for samples produced by spark plasma sintering, with the trace for as-supplied commercial $MgB_2$ powder included for comparison. All observed peaks can be attributed to $MgB_2$, MgO or $MgB_4$.

The MgO content was assessed by XRD as described in section 2. The XRD scans for the samples are shown in figure 3. No phases other than $MgB_2$, MgO and $MgB_4$ were detected. All samples contained MgO and $MgB_4$ in greater amounts than were present in the starting powder. The observed increase in $MgB_4$ content with MgO content is expected if MgO forms from reaction of the Mg vapour, as discussed above. The presence of MgO and $MgB_4$ impurity phases is not uncommon in $MgB_2$ processing, and the relatively high contents of these phases observed in these samples are due to the high processing temperatures used. However, it is likely that this could be reduced by improving the quality of the starting powder, carrying out powder processing in an inert dry atmosphere, or by reducing the processing temperature. This will be possible in future studies as the onset of sintering has observed to occur at temperatures below the peak temperature (figure 2).

The maximum relative density of the samples including the MgO content was calculated using the rule of mixtures, and the results are also shown in Table 1. The density of all the samples relative to the true maximum for the composite samples is

above 90 % indicating significant sintering of the material. The samples produced using 50 MPa and 80 MPa applied uniaxial pressure both had relative densities of 97 %, while the sample produced at the minimum uniaxial pressure was 92 %. This indicates that high uniaxial pressure is a key parameter in producing dense magnesium diboride using SPS, and suggests that there is little additional benefit from using applied pressure above 50 MPa. The relative densities of those samples produced using maximum uniaxial pressures of 50 MPa and above are also significantly higher than those produced by an extensive study of pressureless heat-treatment [20], but approach those of samples produced by HIPing [8-13]. However it is difficult to carry out a direct comparison of these data as it is not always clear whether the impurity content has been taken into account in the determining the sample density.

**Table 1.** Density of $MgB_2$/MgO bulk samples produced using spark plasma sintering in vacuum or argon gas and under a range of uniaxial applied pressures.

| Sample Preparation | MgO Content (wt.% of $MgB_2$ content) | Relative Density (%) |
|---|---|---|
| Vacuum 80 MPa | 8.2 ±1 | 97 ±1 |
| Vacuum 50 MPa | 7.3 ±1 | 97 ±1 |
| Vacuum 16 MPa | 8.6 ±1 | 92 ±1 |

The grain size of all samples prepared in vacuum was measured from polished flat sections using polarised optical microscopy to be around 3 μm. Grains are noticeably elongated with an aspect ratio estimated at approximately 1:2. A typical image is shown in Figure 4.

Samples were also fractured and examined by scanning electron microscopy (Figure 5). Those produced under vacuum using 80 MPa (Figure 5a) and 50 MPa (Figure 5b) maximum uniaxial applied pressures are most similar, consisting of large dense regions with occasional isolated areas of occluded porosity. The sample produced under vacuum using 16 MPa (Figure 5c) uniaxial applied pressure is noticeably more porous, in agreement with the density measurements reported in Table 1.

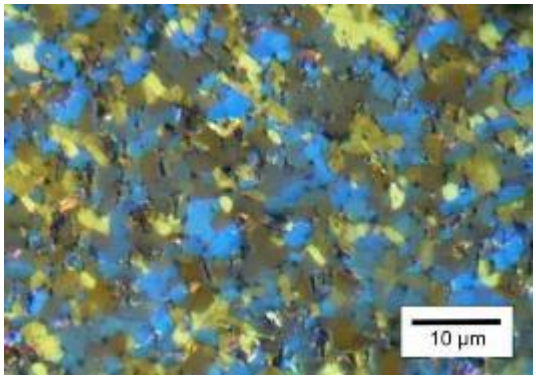


**Figure 4.** Typical polarised optical microscopy image of polished $MgB_2$ bulk sample prepared by spark plasma sintering in vacuum under 50 MPa pressure.

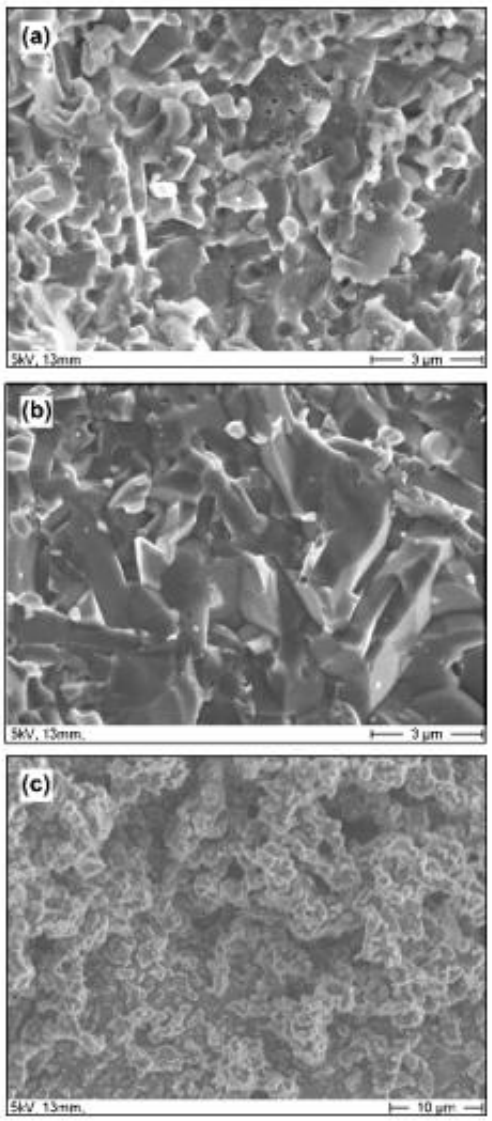


**Figure 5.** Scanning electron micrographs of fracture surfaces of samples prepared by spark plasma sintering under vacuum and maximum applied pressure of a) 80 MPa b) 50 MPa and c) 16 MPa.

The hardness of the samples was measured using Vickers indentation, and the average hardness for each sample is given in Table 2. Samples prepared in vacuum at the higher uniaxial pressures had Vickers hardness values above 1000 HV, suggesting a well-sintered ceramic microstructure. In comparison, dense HIPed samples prepared under 3.5 GPa had Vickers hardness values of 1700–2800 HV [8] and porous samples produced by pressureless heat-treatment [20] had Vickers hardness values of 35–90 HV.

Using data from our previous work on $MgB_2$ bulks produced using pressureless heat-treatment and resistive sintering [20], we can demonstrate for the first time a correlation between density and hardness for $MgB_2$ (Figure 6). This relationship is monotonic up to around 1200 HV, indicating that at high density and hardness other factors such as grain size may affect the relationship between the variables. A very similar correlation between density and hardness has been established by Mukhopadhyay *et al* for sialon materials [23], indicating that in this respect $MgB_2$

exhibits the sintering behaviour expected of classical structural ceramics. The establishment of this correlation may be useful for samples for which the density is difficult to determine.

**Table 2.** Hardness of magnesium diboride bulks produced by spark plasma sintering. Errors are calculated from the standard deviation of 10 measurements on each sample.

| Sample Preparation | Vickers Hardness (HV/2) | Vickers Hardness (GPa) |
|---|---|---|
| Vacuum 80 MPa | 1050 ± 20 | 10.3 ± 0.2 |
| Vacuum 50 MPa | 1110 ± 10 | 10.9 ± 0.1 |
| Vacuum 16 MPa | 658 ± 9 | 6.45 ± 0.1 |
| Ar gas 80 MPa | 323 ± 10 | 3.17 ± 0.1 |

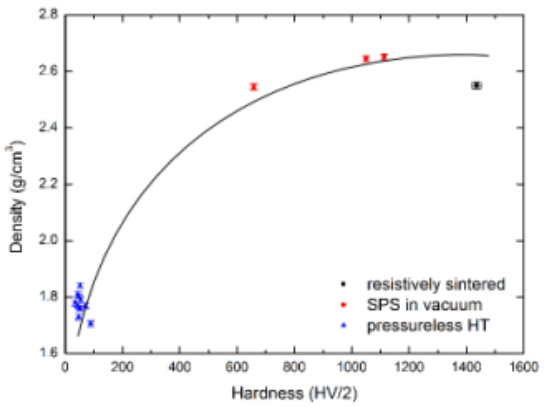


**Figure 6.** Correlation between hardness and density for magnesium diboride bulks, using data from this work (SPS) and from [20] (pressureless HT and resistive sintered).

### 3.1 Superconducting Properties

The superconducting properties of the bulk samples were measured by the magnetization method using a VSM. $T_{c,onset}$ was measured as approximately 32 K using the AC susceptibility method in a magnetic field of 0.5 T. The depression of $T_{c,onset}$ when measured in a magnetic field of 0.5 T is expected; comparison with Frederick *et al* [24] indicates that carrying out measurements at 1 T would be expected to reduce $T_{c,onset}$ by around 5 K compared to the value at 0 T.

In measurements carried out at 4 K on the sample prepared at higher pressure some jumps in the magnetization loops were seen due to flux jumping (figure 7), similar to those seen by Yanmaz et al [25], Miu et al [26] and Goeckner et al [27]. In this particular data set, these jumps occur at −1.4, −0.12, 0.0067 and 1.3 T and are thought to be sensitive to the magnetic sweep rate [25]. No jumps were seen in the data recorded at 20 K.

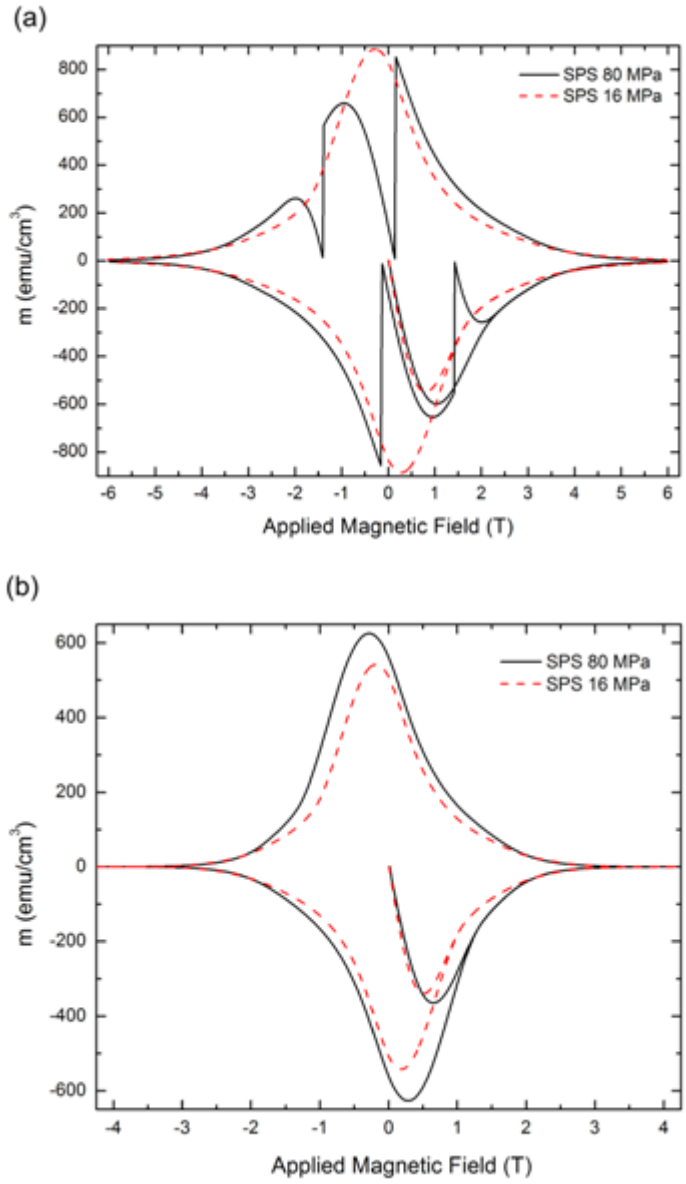


**Figure 7.** Magnetization loops recorded for samples prepared by spark plasma sintering in vacuum under 16 MPa and 80 MPa maximum applied uniaxial pressure. Magnetization measurements carried out at a) 4 K and b) 20 K.

The critical current density $J_{c,mag}$ was calculated from the magnetization data using the Bean model [28] and plotted against applied magnetic field (figure 8). The regions where flux jumps were observed in the M–H loop were not used for these calculations. These data are compared to those associated with an $MgB_2$ bulk sample produced for an earlier study by pressureless heat-treatment under Ar gas at 1100 ◦C [20]. This data was measured using a quantum design magnetic property measurement system with 7 T field. The pressureless heat-treated sample has a relative density of around 65% and hardness of 90 HV, and contains approximately 7 wt% MgO following heat-treatment. It is evident that $J_{c,mag}$ is consistently higher across the range of magnetic fields for the spark plasma sintered bulks than for that produced by pressureless heat-treatment at both 4 and 20 K, with the steeper gradient of the curves indicative of poorer connectivity in the pressureless heat-treated sample. This indicates the positive effect of densification on the superconducting properties of

$MgB_2$ bulks. The $J_{c,mag}$ versus T curves of the samples prepared by SPS at 16 and 80 MPa are similar, suggesting that full densification is not necessary to optimize this improvement. Figure 5 suggests that grain growth begins to accelerate as pinning of grain boundaries by pores diminishes. It is possible that the negative effect on $J_{c,mag}$ due to the increased grain size for the denser samples negates the benefits of increased densification.

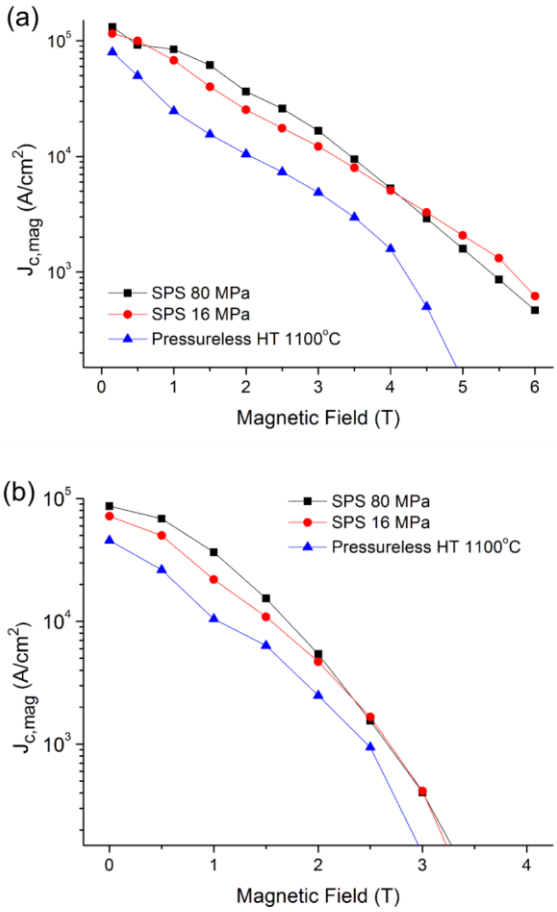


**Figure 8.** Variation of critical current density with applied magnetic field for spark plasma sintered samples prepared in vacuum as measured by magnetisation method and calculated using the Bean Model at constant temperatures of a) 4 K and b) 20 K.

There is surprisingly little comparable data in the literature for $J_{c,mag}$ measurements on dense ex situ bulks. Hot pressed samples studied by Hsieh *et al* [14] have almost identical $J_{c,mag}$ values to our spark plasma sintered samples at 20 K up to 2 T and have similar gradients above 2.5 T. The best Jc,mag values in the literature for comparable samples are around $1 \times 10^6$ A cm$^{-2}$ at 0 T for bulks produced by hot isostatic pressing under moderate pressures of 100–200 MPa (processing temperatures of 775, 950 and 1000 ◦C) [8, 11]. We speculate that the higher critical current density may be due to the fact that either grain growth has not occurred or the size and distribution of defects such as impurity phases may result in enhanced pinning in these samples, but the necessary microstructural data is not available in the literature to test this hypothesis.

## 4. Conclusions

Dense magnesium diboride bulks were prepared by spark plasma sintering using systematically varied pressure and atmosphere in order to study the effect of these variables on the final microstructure and superconducting properties. Dilatometric data recording the change in the sample density collected during the heat-treatment reveals the relationship between temperature, pressure and densification. The onset of sintering, determined from the dilatometric data, consistently occurs above 1000$^{o}$C (in agreement with Tampieri *et al* [15]) regardless of the applied pressure. This temperature is above that typically used in the production of *ex situ* magnesium diboride wires and tapes, which is generally around 850-950$^{o}$C [29] due to deleterious reactions of the sheath material with the magnesium diboride core, which severely reduce the superconducting cross-section of the wire [30]. Further studies on the effect of lowering the spark plasma sintering temperature below that used in this study would establish whether there is a narrow processing window in which well-sintered $MgB_2$ cores in wires can be produced.

Calculations of the bulk density, taking into account the impurity content, indicated that bulks prepared in vacuum using applied uniaxial pressure of 50 MPa or above were almost fully dense (97%) while a bulk prepared using the minimum possible applied pressure (16 MPa) had a significantly lower density at 92 %. These results indicate the importance of applied pressure in production of dense magnesium diboride bulks. Following heat-treatment, x-ray diffraction spectra of magnesium diboride bulk prepared in argon gas showed MgO as the majority phase whereas those samples prepared in vacuum contained less than 9 wt% MgO.

Using measurements of Vickers hardness and density carried out on these spark plasma sintered samples and on more porous magnesium diboride bulks prepared by pressureless heat-treatment at a range of temperatures, we have established a correlation between these two variables and suggest that this will be useful in assessing the density of samples where the density is difficult to measure by Archimedes' method. In addition, higher $J_{c,mag}$ values calculated from magnetization data indicate that the connectivity in the spark plasma sintered samples is improved compared to that of the samples prepared by pressureless heat-treatment, in agreement with the observations of Liao et al [31]. The similarity of $J_{c,mag}$ values for samples of 92% and 97% relative density indicates that once the density is above around 90% the critical current density is strongly influenced by other mechanisms such as grain growth.

## Acknowledgements

CEJD gratefully acknowledges funding from the EPSRC through the University of Oxford Department of Materials 2004 Doctoral Training Grant.

## References

[1] Nagamatsu J, Nakagawa N, Muranaka T, Zenitani Y and Akimitsu J 2001 *Nature* **410** 63
[2] Buzea C and Yamashita T 2001 *Superconductor Science and Technology* **14** R115
[3] Flukiger R, Suo H L, Musolino N, Beneduce C, Toulemonde P and Lezza P 2003 *Physica C* **385** 286
[4] Goldacker W, Schlachter S I, Liu B, Obst B and Klimenko E 2004 *Physica C* **401** 80
[5] Zhou S, Pan A V, Liu H and Dou S 2002 *Physica C* **382** 349

[6] Penco R and Grasso G 2007 *IEEE Transactions on Applied Superconductivity* **17** 2291
[7] Grinenko V, Krasnoperov E P, Stoliarov C A, Bush A A and Mikhajlov B P 2006 *Solid State Communications* **138** 461
[8] Takano Y, Takeya H, Fujii H, Kumakura H, Hatano T, Togano K, Kito H and Ihara H 2001 *Applied Physics Letters* **78** 2914
[9] Indrakanti S S, Nesterenko V F, Maple M B, Frederick N A, Yuhasz W H and Li S 2001 *Philosophical Magazine Letters* **81** 849
[10] Maple M B, Taylor B J, Frederick N A, Li S, Nesterenko V F, Indrakanti S S and Maley M P 2002 *Physica C* **382** 132
[11] Shields T C, Kawano K, Holden D and Abell J S 2002 *Superconductor Science and Technology* **15** 202
[12] Sung G Y, Kim S H, Kim J, Yoo D C, Lee J W, Lee J Y, Jung C U, Park M S, Kang W N N, Du Z L and Lee S I 2001 *Superconductor Science and Technology* **14** 880
[13] Jung C U, Park M S, Kang W N, Kim M S, Lee S Y and Lee S I 2001 *Physica C* **353** 162
[14] Hsieh C H, Chang C H, Chang C N, Sou U C, Sheu H S, Hsu H C and Yang H C 2006 *Solid State Communications* **137** 97
[15] Tampieri A, Celotti G, Sprio S, Caciuffo R and Rinaldi D 2004 *Physica C* **400** 97
[16] Kumakura H, Takano Y, Fujii H, Togano K, Kito H and Ihara H 2001 *Physica C* **363** 179
[17] Lee S Y, Yoo S I, Kim Y W, Hwang N M and Kim D Y 2003 *Journal of the American Ceramic Society* **86** 1800
[18] Schmidt J, Schnelle W, Grin Y and Kniep R 2003 *Solid State Sciences* **5** 535
[19] Shim S H, Shim K B and Yoon J W 2005 *Journal of the American Ceramic Society* **88** 858
[20] Dancer C E J, Mikheenko P, Bevan A I, Abell J S, Todd R I and Grovenor C R M *Journal of the European Ceramics Society* **29** 1817
[21] Reed J 1982 *Principles of Ceramic Processing* (New York:Wiley-Interscience)
[22] Kim S, Stone D S, Cho J-I, Jeong C-Y, Kang C-S and Bae J-C 2009 J. Alloys Compounds **470** 85
[23] Mukhopadhyay A, Datta S and Chakraborty D 1991 *Ceramics International* **17** 121
[24] Frederick N A, Li S, Maple M B, Nesterenko V F and Indrakanti S S 2001 *Physica C* **363** 1
[25] Yanmaz E, Savaskan B, Basoglu M, Taylan Koparan E, Dilley N R and Grovenor C R M 2009 J. Alloys Compounds **480** 203
[26] Miu L, Ivan I, Aldica G, Badica P, Groza J R, Miu D, Jakob G and Adrian H 2008 *Physica C* **468** 2279
[27] Goeckner H P, Claus H and Kouvel J S 2005 Physica C **418** 93
[28] Bean C. 1964 *Reviews of Modern Physics* **36** 31
[29] Flukiger R, Suo H L, Musolino N, Beneduce C, Toulemonde P and Lezza P 2003 *Physica C* **385** 286
[30] Grovenor C R M, Goodsir L, Salter C J, Kovac P and Husek I 2004 *Superconductor Science and Technology* **17** 479
[31] Liao X Z, Serquis A, Zhu Y T, Civale L, Hammon D L, Peterson D E, Mueller F M, Nesterenko V F, Gu Y 2003 *Superconductor Science and Technology* **16** 799